



**HAL**  
open science

## Hippocampal T cell infiltration promotes neuroinflammation and cognitive decline in a mouse model of tauopathy

Cyril Laurent, Guillaume Dorothee, Stéphane Hunot, Elodie Martin, Yann Monnet, Marie Duchamp, Yuan Dong, François-Pierre Légeron, Antoine Leboucher, Sylvie Burnouf, et al.

### ► To cite this version:

Cyril Laurent, Guillaume Dorothee, Stéphane Hunot, Elodie Martin, Yann Monnet, et al.. Hippocampal T cell infiltration promotes neuroinflammation and cognitive decline in a mouse model of tauopathy. *Brain - A Journal of Neurology* , 2017, 140 (1), pp.184 - 200. 10.1093/brain/aww270 . inserm-01833350

**HAL Id: inserm-01833350**

**<https://inserm.hal.science/inserm-01833350v1>**

Submitted on 6 Dec 2023

**HAL** is a multi-disciplinary open access archive for the deposit and dissemination of scientific research documents, whether they are published or not. The documents may come from teaching and research institutions in France or abroad, or from public or private research centers.

L'archive ouverte pluridisciplinaire **HAL**, est destinée au dépôt et à la diffusion de documents scientifiques de niveau recherche, publiés ou non, émanant des établissements d'enseignement et de recherche français ou étrangers, des laboratoires publics ou privés.



Distributed under a Creative Commons Attribution 4.0 International License

# Hippocampal T cell infiltration promotes neuroinflammation and cognitive decline in a mouse model of tauopathy

Cyril Laurent,<sup>1</sup> Guillaume Dorothee,<sup>2,3,\*</sup> Stéphane Hunot,<sup>4,5,6,7,\*</sup> Elodie Martin,<sup>4,5,6,7,\*</sup> Yann Monnet,<sup>4,5,6,7</sup> Marie Duchamp,<sup>2,3</sup> Yuan Dong,<sup>2,3</sup> François-Pierre Légeron,<sup>4,5,6,7</sup> Antoine Leboucher,<sup>1</sup> Sylvie Burnouf,<sup>1</sup> Emilie Faivre,<sup>1</sup> Kévin Carvalho,<sup>1</sup> Raphaëlle Caillierez,<sup>1</sup> Nadège Zommer,<sup>1</sup> Dominique Demeyer,<sup>1</sup> Nathalie Jouy,<sup>1,8</sup> Veronique Sazdovitch,<sup>4,5,9</sup> Susanna Schraen-Maschke,<sup>1</sup> Cécile Delarasse,<sup>4,5,6,7</sup> Luc Buée<sup>1,#</sup> and David Blum<sup>1,#</sup>

\*,# These authors contributed equally to this work.

Alzheimer's disease is characterized by the combined presence of amyloid plaques and tau pathology, the latter being correlated with the progression of clinical symptoms. Neuroinflammatory changes are thought to be major contributors to Alzheimer's disease pathophysiology, even if their precise role still remains largely debated. Notably, to what extent immune responses contribute to cognitive impairments promoted by tau pathology remains poorly understood. To address this question, we took advantage of the THY-Tau22 mouse model that progressively develops hippocampal tau pathology paralleling cognitive deficits and reappraised the interrelationship between tau pathology and brain immune responses. In addition to conventional astroglial and microglial responses, we identified a CD8-positive T cell infiltration in the hippocampus of tau transgenic mice associated with an early chemokine response, notably involving CCL3. Interestingly, CD8-positive lymphocyte infiltration was also observed in the cortex of patients exhibiting frontotemporal dementia with P301L tau mutation. To gain insights into the functional involvement of T cell infiltration in the pathophysiological development of tauopathy in THY-Tau22 mice, we chronically depleted T cells using anti-CD3 antibody. Such anti-CD3 treatment prevented hippocampal T cell infiltration in tau transgenic animals and reverted spatial memory deficits, in absence of tau pathology modulation. Altogether, these data support an instrumental role of hippocampal T cell infiltration in tau-driven pathophysiology and cognitive impairments in Alzheimer's disease and other tauopathies.

1 Univ. Lille, Inserm, CHU-Lille, UMR-S 1172, Alzheimer and Tauopathies, Lille, France

2 INSERM, UMRS 938, CdR Saint-Antoine, Laboratory Immune System, Neuroinflammation and Neurodegenerative Diseases, Hôpital St-Antoine, Paris, France

3 Sorbonne Universités, UPMC Univ Paris 06, UMRS 938, CdR Saint-Antoine, Hôpital Saint-Antoine, Paris, France

4 Inserm, U 1127, F-75013, Paris, France

5 CNRS, UMR 7225, F-75013, Paris, France

6 Sorbonne Universités, UPMC Univ Paris 06, UMR S 1127, F-75013, Paris, France

7 Institut du Cerveau et de la Moelle épinière, ICM, F-75013, Paris, France

8 BioImaging center of Lille, 59045 Lille, France

9 Laboratoire de Neuropathologie Escourrolle, Hôpital de la Salpêtrière, AP-HP, Paris, France

Correspondence to: Dr David Blum

Inserm UMR-S1172, 'Alzheimer and Tauopathies', Place de Verdun, 59045, Lille Cedex, France

E-mail: david.blum@inserm.fr

Received March 29, 2016. Revised August 28, 2016. Accepted September 5, 2016. Advance Access publication November 5, 2016

© The Author (2016). Published by Oxford University Press on behalf of the Guarantors of Brain.

This is an Open Access article distributed under the terms of the Creative Commons Attribution Non-Commercial License (<http://creativecommons.org/licenses/by-nc/4.0/>), which permits non-commercial re-use, distribution, and reproduction in any medium, provided the original work is properly cited. For commercial re-use, please contact [journals.permissions@oup.com](mailto:journals.permissions@oup.com)

**Keywords:** tauopathy; T cells; neuroinflammation; chemokines; frontotemporal lobar degeneration

**Abbreviations:** IgG = immunoglobulin G; IFN $\gamma$  = interferon- $\gamma$ ; TCR = T cell receptor; TNF $\alpha$  = tumor necrosis factor  $\alpha$

## Introduction

Alzheimer's disease is a neurodegenerative disorder characterized by the progressive development of memory deficits. Its neuropathology is defined by extracellular accumulation of amyloid- $\beta$  peptides into amyloid plaques and intraneuronal fibrillar aggregates of hyper- and abnormally phosphorylated tau proteins (Masters *et al.*, 1985; Sergeant *et al.*, 2008). Lesions in Alzheimer's disease lead to activation of microglial and astroglial cells, triggering a chronic neuroinflammatory innate immune response. Contribution of such neuroinflammation to the pathophysiology of Alzheimer's disease remains highly debated, with both beneficial impacts and detrimental effects that may promote the neurodegenerative process (for review see Heneka *et al.*, 2015). Finally, recent genetic evidence also supported a role of innate immune system in Alzheimer's disease aetiology (Guerreiro *et al.*, 2013; Lambert *et al.*, 2013).

Besides innate neuroinflammation, accumulating evidence emphasizes the involvement of cellular adaptive immunity in the pathophysiology of Alzheimer's disease. Polymorphisms in genes associated with antigen presentation to T cells were identified as susceptibility loci for Alzheimer's disease (Jones *et al.*, 2010; Lambert *et al.*, 2010, 2013). In addition, increased T cell infiltration in the brain parenchyma and enhanced peripheral T cell responses to amyloid- $\beta$  have previously been described in patients with Alzheimer's disease (Rogers *et al.*, 1988; Togo *et al.*, 2002; Monsonogo *et al.*, 2003). Of note, higher proportion of activated CD8<sup>+</sup> T cells in the CSF of patients correlated with clinical and structural markers of the pathology (Lueg *et al.*, 2015). Finally, previous reports in mouse models developing amyloid pathology suggested that different types of amyloid- $\beta$ -specific CD4<sup>+</sup> T cells might either promote both enhanced amyloid- $\beta$  clearance and encephalitis, or reverse cognitive decline and synaptic loss (Ethell *et al.*, 2006; Monsonogo *et al.*, 2006; Cao *et al.*, 2009). However, the role of T cells in Alzheimer's disease pathophysiology remains largely ill-defined.

Whereas most studies investigating the role of innate neuroinflammation or adaptive immunity in Alzheimer's disease were carried out in the context of amyloid pathology, much less is known regarding brain immune responses associated with tauopathy. In Alzheimer's disease, tau pathology is observed early in the brainstem and entorhinal cortex (Braak *et al.*, 2011). Its progression from entorhinal cortex to hippocampus and lastly neocortex is associated with progression of clinical symptoms (Duyckaerts *et al.*, 1997; Delacourte *et al.*, 1999; Grober *et al.*, 1999), supporting a pivotal role of tau pathology in cognitive deficits. In accordance, tau pathology has been associated with hippocampal synaptic impairments and

memory deficits in tau transgenic models (Burnouf *et al.*, 2013; Ahmed *et al.*, 2015). To what extent immune responses may contribute to tau-triggered cognitive decline in Alzheimer's disease remains poorly understood. Previous studies largely focused on the role of glial cells, showing that tau pathology is prone to activate microglia and astrocytes (Bellucci *et al.*, 2004; Sasaki *et al.*, 2008; Belarbi *et al.*, 2011). In a detrimental circle, microglia activation was suggested to play an important role in the development/spreading of tau pathology and associated memory deficits (Yoshiyama *et al.*, 2007; Gorlovoy *et al.*, 2009; Bhaskar *et al.*, 2010; Nash *et al.*, 2013; Asai *et al.*, 2015). In sharp contrast, the link between tau-related pathology and T cell responses remains totally unknown.

In the present study, we sought to investigate the relationships between tau pathology and brain innate and cellular adaptive immunity using the THY-Tau22 mouse model, which progressively develops hippocampal tauopathy and spatial memory deficits (Burnouf *et al.*, 2013; Laurent *et al.*, 2016). In addition to the expected activation of microglia and astrocytes, our data demonstrate that hippocampal tau pathology is associated with chemokine production and parenchymal T cell infiltration. Importantly, T cell depletion improved spatial memory of THY-Tau22 mice, suggesting an instrumental role of cellular adaptive immunity into tau-triggered cognitive deficits in Alzheimer's disease.

## Materials and methods

### Animals and study design

THY-Tau22 mice (C57BL/6J background) were generated by overexpression of human four-repeat tau mutated at sites G272V and P301S under the control of the neuronal Thy1.2 expression cassette (Schindowski *et al.*, 2006). Non-transgenic wild-type littermates were used as controls. Mice were housed (four to six per cage) in a specific and opportunistic pathogen-free facility and maintained on a 12-h light-dark cycle with *ad libitum* access to food and water. Providing no major gender-related differences were demonstrated in THY-Tau22 mice (Laurent *et al.*, 2016; data not shown), in the present study, both males and females were used for the characterization of immune responses and females to study the effect of anti-CD3 treatment.

Characterization of hippocampal neuroinflammatory responses in THY-Tau22 animals was carried out from 3 months of age (early disease stages) to 12 months of age, when tau pathology and memory deficits are maximal in this model (Burnouf *et al.*, 2012; Van der Jeugd *et al.*, 2013). For such characterization, some of the mice were sacrificed by cervical dislocation, brains harvested and hippocampi dissected out using a coronal acrylic slicer (Deltamicroscopies) at 4°C

and stored at  $-80^{\circ}\text{C}$  for biochemical and mRNA analyses. Mice used for immunohistochemical studies were transcardially perfused with NaCl 0.9% and paraformaldehyde 4%, brains were harvested, post-fixed for 24 h in paraformaldehyde 4% and cryoprotected in 20% sucrose before being frozen.

Contribution of T cells to the pathophysiological development in THY-Tau22 mice was investigated following intraperitoneal administration (5 mg/kg every 2 weeks) of depleting hamster anti-mouse CD3 $\epsilon$  monoclonal IgG1 antibody (clone 145-2C11; BioXcell BE0001-1) or hamster IgG isotype control (BioXcell BE0091) (BioXCell). A total of 58 animals were assigned to balanced groups (wild-type iso, wild-type anti-CD3, Tau22 iso and Tau22 anti-CD3). Body weight was measured all along the protocol for monitoring healthy condition of animals (not shown). Blood was collected by tail vein sampling, and flow cytometry analyses were carried out for monitoring treatment efficiency and specificity. T cell depletion was initiated at 4 months of age, i.e. before lymphocyte infiltration was detected, and maintained until 9 months of age, when transgenic animals exhibit maximal T cell recruitment (Fig. 3). At completion of anti-CD3 experiment, half of the animals were transcardially perfused as indicated above. Hippocampi from remaining brains were dissected out for later biochemical analyses. All protocols involving animal studies were approved by local ethics committee (agreement n $^{\circ}$ CEEA 062010R).

## CD8 immunohistochemistry in post-mortem brain of patients exhibiting frontotemporal dementia with P301L mutation

Experiments using human post-mortem material were approved by the ‘Comité de Protection des Personnes’ review board (Ile de France 1, Paris, France). Immunohistochemical staining on human brain was performed on autopsy cortical tissue (temporal) from three control subjects and three patients with frontotemporal dementia and P301L tau mutation (Papegaye *et al.*, 2016). Tissue was fixed in formaldehyde and then embedded in paraffin. Paraffin-embedded tissues were cut in serial 8  $\mu\text{m}$  thick slices on a microtome, and sections were recovered on SuperFrost $^{\text{®}}$  Plus slides (Kindler O GmbH), before incubation at  $56^{\circ}\text{C}$  for 3 days. Diseased individuals and control subjects did not differ in terms of their mean age at death [frontotemporal patients,  $58 \pm 7.5$  years of age; controls  $65 \pm 6$  years of age;  $P = 0.5$ , Student’s *t*-test; mean  $\pm$  standard error of the mean (SEM)] or the mean interval from death to the freezing of tissue (frontotemporal patients,  $18.0 \pm 9.8$  h; controls  $22.0 \pm 7.5$  h;  $P = 0.78$ ; Student’s *t*-test; mean  $\pm$  SEM).

Immunohistochemistry was performed using the Ventana BenchMark LT (Ventana Medical System Inc.). The fully automated processing of barcode-labelled slides included baking of the slides, solvent-free deparaffinization and 30 min of CC1 (Tris/EDTA buffer pH 8.0) antigen retrieval. Human slides were incubated with primary antibody directed against CD8 (clone C8/144B; mouse monoclonal IgG1; dilution 1/25, Dako) for 32 min at room temperature. Staining was revealed by the ABC method (Vector Laboratories) with

3,3-diaminobenzidine as the peroxidase substrate and sections were counterstained with haematoxylin and eosin solution.

## Mouse tissue immunostainings

For immunohistochemical staining, 40  $\mu\text{m}$  floating sections were incubated with primary antibodies directed against Mac-1/CD11b (clone 5C6; rat monoclonal IgG2b; dilution 1/250, AbD Serotec), GFAP (rabbit polyclonal Ig fraction; dilution 1/4000; Dako Z0334;), CD8 $\alpha$ , (clone KT15; rat monoclonal IgG2a; dilution 1/100; AbD Serotec) or CD4 (clone YTS191.1; rat monoclonal IgG2a; dilution 1/100, AbD Serotec), at  $4^{\circ}\text{C}$  for 24 to 48 h. Staining was revealed by the ABC method (Vector Laboratories) with 3,3'-diaminobenzidine as the peroxidase substrate.

For immunofluorescent stainings, brain sections were incubated with the following primary antibodies directed against zonula occludens-1 (rabbit polyclonal Ig fraction; dilution 1/500; Zymed), occludin (rabbit polyclonal Ig fraction; dilution 1/500; Zymed), von Willebrand factor (mouse monoclonal clone G-11; dilution 1/200; Santa Cruz). Appropriate Alexa Fluor $^{\text{®}}$  488- and Alexa Fluor $^{\text{®}}$  568-conjugated secondary antibodies (Invitrogen) were incubated for 1 h at room temperature at 1:1000 dilution to reveal the primary antibodies. Sections were counterstained and mounted with Vectashield/DAPI (Vector). Images were acquired on a LSM 710 confocal laser-scanning confocal microscope (Carl Zeiss).

For CCL3 immunofluorescence, brain sections were simultaneously incubated for 48 h at  $4^{\circ}\text{C}$  with two primary antibodies developed in different species and diluted in PBS 0.1 M plus 0.1% Triton $^{\text{TM}}$  X-100: anti-CCL3 (AF-450-NA; Goat IgG; dilution 1:100; R&D Systems) and anti-Iba1 (019-19741; rabbit polyclonal; dilution 1/500; Wako) or anti-GFAP (Z0334; rabbit polyclonal; dilution 1/500; Dako). Appropriate donkey Alexa Fluor $^{\text{®}}$  488- and Alexa Fluor $^{\text{®}}$  647-conjugated secondary antibodies (Life Technologies) were incubated for 1 h at room temperature at 1/1000 dilution to reveal the primary antibodies. DAPI counterstaining (Invitrogen, P36931, dilution 1/1000, 5-min incubation) was performed to reveal nuclei. Sections were examined with an upright confocal microscope Olympus FV-1000 using Olympus FV-1000 software. Images were then prepared with ImageJ software. Noteworthy, specificity of CCL3 immunostaining was validated using immunoabsorption and use of CCL3 knockout mice (not shown).

For IgG immunofluorescence, brain sections were incubated for 1 h at room temperature with antibody directed against total mouse IgG (Alexa Fluor $^{\text{®}}$  488-conjugated goat anti-mouse IgG, 1/500; Life technologies). Sections were counterstained and mounted with Vectashield/DAPI (Vector). Images were acquired with an Apotome microscope (Imager Z1; Zeiss).

## Y-maze studies

Short-term spatial memory was assessed in a spontaneous novelty-based spatial preference Y-maze test as previously described (Laurent *et al.*, 2016). Each arm of the Y-maze was 22-cm long, 6.4-cm wide, with 15-cm high opaque walls. Different extramaze cues were placed on the surrounding walls. Sawdust was placed in the maze during the experiments and mixed between each phase. Allocation of arms was

counterbalanced within each group. During the exposure phase, mice were placed at the end of the ‘start’ arm and were allowed to explore the ‘start’ arm and the ‘other’ arm for 5 min (beginning from the time the mouse first left the start arm). Access to the third arm of the maze (‘novel’ arm) was blocked by an opaque door. The mouse was then removed from the maze and returned to its home cage for 2 min. In the test phase, the mouse was placed again in the ‘start’ arm of the maze, the door of the ‘novel’ arm was removed and the mouse was allowed to explore the maze for 5 min (from the time the mouse first left the start arm). The amount of time the mouse spent in each arm of the maze was recorded during both exposure and test phases using EthovisionXT (Noldus Information Technology).

## mRNA extraction and quantitative real-time reverse transcription polymerase chain reaction

Total RNA were extracted from hippocampi and purified using the RNeasy<sup>®</sup> Lipid Tissue Mini Kit (Qiagen). One microgram of total RNA was reverse-transcribed using the High-Capacity cDNA reverse transcription kit (Applied Biosystems). Quantitative real-time reverse transcription polymerase chain reaction (RT-PCR) analysis was performed on an Applied Biosystems Prism 7900 System using Power SYBR<sup>®</sup> Green PCR Master Mix (Applied Biosystems). The thermal cycler conditions were as follows: 95°C for 10 min, then 45 cycles at 95°C for 15 s and 60°C for 25 s. Sequences of primers used in this study are given in Supplementary Table 1. Cyclophilin A (*Ppia*) was used as a reference housekeeping gene for normalization. Amplifications were carried out in triplicate and the relative expression of target genes was determined by the  $\Delta\Delta C_t$  method.

## Microarray study and GO term enrichment

RNA quality was checked on RNA 6000 Nano chips using a Bioanalyser 2100 (Agilent Technologies). RNA samples used for microarray experiments had RNA integrity numbers (RINs) > 8.3. Agilent’s Quick Amp labelling Kit (One-color) was used to generate fluorescent cRNA. The amplified cyanine 3-labelled cRNA samples were then purified using Qiagen’s RNeasy<sup>®</sup> mini spin columns and hybridized to Agilent Whole Mouse Genome Microarrays, 4x44K microarray. Slides were washed and scanned with the Agilent scanner G2505C, according to manufacturer’s standard protocol. Information from probe features was extracted from microarray scan images using the Agilent Feature Extraction software v.10.5.1.1. Analyses were performed using GeneSpring 10.0 (Agilent Technologies). Normalization between arrays was performed using the 75 percentile method, flagged probes and low intensity ones in both conditions were removed from statistical analysis. Student *t*-test was performed with Benjamini-Hochberg multiple testing correction as implemented in GeneSpring 10.0 with a *P*-value cut-off of 0.05. Finally we applied a fold change threshold of 2 and found 32 2-fold differentially expressed genes. We carried out a (Gene Ontology) GO-term enrichment analysis for the 32

differentially expressed genes using AmiGO (version 1.7) and MGI as a reference database (GO database release 2010-02-08), with a minimum number of gene products of 2 and a 0.01 *P*-value cut-off with Bonferroni correction. Three genes were excluded from the GO-term enrichment analysis because of their exclusion from the GO database.

## Biochemical studies

Tissue was homogenized in 200  $\mu$ l Tris buffer (pH 7.4) containing 10% sucrose and protease inhibitors (Complete; Roche Diagnostics), sonicated and kept at  $-80^{\circ}\text{C}$  until use. Protein amounts were quantified using the BCA assay (Pierce), and samples diluted with lithium dodecyl sulphate buffer (2 $\times$ ) supplemented with reducing agents (Invitrogen) and then separated on 4–12% NuPAGE<sup>®</sup> Novex gels (Invitrogen). Proteins were transferred to nitrocellulose membranes, which were then saturated with 5% non-fat dried milk or 5% bovine serum albumin in TNT (Tris 15 mM pH 8, NaCl 140 mM, 0.05% Tween) and incubated at 4°C for 24 h with the primary antibodies directed against phosphoepitope of tau protein as follows: phospho(p)-Tyr18, pThr212/pSer214 (AT100) (Pierce), pSer262, pSer404, pSer422 (Invitrogen); dephosphorylated tau (Tau1, Millipore), total tau Cter (in-house antibody recognizing the 11 amino acids in COOH-terminal part of tau), HT7 (MN1000, Thermo Scientific). We also used anti-Arc (SantaCruz, sc17839) and anti 14-3-3 (Santa Cruz, 1019) antibodies. Appropriate HRP-conjugated secondary antibodies were incubated for 1 h at room temperature and signals were visualized using chemoluminescence kits (ECL, Amersham Bioscience) and a LAS4000 imaging system (Fujifilm). Results were normalized to actin and quantifications were performed using ImageJ software (Scion Software).

## ELISA

Hippocampal tissues were homogenized in RIPA buffer (Tris HCl 25 mM, NaCl 150 mM, NP40 1%, sodium deoxycholate 1%, SDS 0.1%, pH 7.6). The resulting lysates were sonicated and incubated for 1 h at 4°C under agitation before centrifugation (12 000 g, 4°C, 15 min). Supernatants were collected and protein amounts determined using the BCA assay (Pierce). CCL3, CCL4 and CCL5 levels were quantified using commercially available ELISA assays (R&D Systems) after loading 300  $\mu$ g of proteins in 50  $\mu$ l volume.

## Isolation of brain-myeloid cells

Preparation of CNS-immune cells was performed using Percoll<sup>®</sup> separation as described previously (Fazilleau *et al.*, 2007). Briefly, mice were perfused with phosphate-buffered saline (PBS) and the brains were dissected out and homogenized in 5 ml of PBS with collagenase IV at 0.2 mg/ml and DNase I at 1 mg/ml (both from Sigma-Aldrich) for 30 min at 37°C and 5% CO<sub>2</sub>. The brain homogenate was washed with PBS-foetal bovine serum 5% and centrifuged in a 30/37/70% Percoll<sup>®</sup> gradient (GE Healthcare). Myeloid cells were recovered from the 37/70% Percoll<sup>®</sup> interphase and washed. The pellet containing the myeloid cells was resuspended in 400  $\mu$ l PBS-bovine serum albumin 0.5%. Binding of antibodies to Fc receptors was prevented by adding 1  $\mu$ g Fc-block (anti-CD16/CD32 antibodies). One hundred microlitres of cells were

labelled with 100  $\mu$ l of primary antibodies mix: anti-CD45-V450 (30F11) (BD Biosciences) and anti-CD11b-PerCPCy5.5 (M1/70) (eBioscience). After labelling, cells were fixed in 1% paraformaldehyde. A logical gate strategy was applied for the fluorescence-activated cell sorting (FACS) experiments: a morphological gating referred to dot plot FSC-Area versus SSC-Area and duplets discrimination referred to dot plot FSC-Area versus FSC-Height. To standardize our FACS analyses, we analysed the same number of cells for each sample *i.e.* 20 000 events in this gate per sample. For compensation settings, compbeads (BD Biosciences) with corresponding antibodies were used. Fluorescence intensities were measured using a FACS Verse analyser (BD Biosciences) and data were analysed using the FlowJo Software (FlowJo LLC).

## T cell analyses

Efficiency and specificity of T cell depletion was monitored by flow cytometry. B and T lymphocytes were quantified in blood samples the day before and 5 days after anti-CD3 or isotype control administration. Cells were first incubated for 10 min with FcR-blocking antibodies (2.4G2; BD Biosciences) to avoid non-specific staining, and then surface stained with phycoerythrin-conjugated anti-CD19 (1D3; BD Biosciences) and allophycocyanin-conjugated anti-TCR $\beta$  (H57-597; BD Biosciences) antibodies. In a pilot cohort, 5 days after treatment completion single-cell suspensions were prepared from spleen and pooled popliteal, cervical, inguinal and mesenteric lymph nodes, and then analysed similarly.

In other experiments, we carried out a detailed phenotypic analysis of both CD8<sup>+</sup> and CD4<sup>+</sup> peripheral T cells in the blood, spleen and pooled lymph nodes from 5/6-month-old wild-type and THY-Tau22 mice. Cells were first incubated with FcR blocking antibody (2.4G2; BD Biosciences) to avoid non-specific staining. Anti-CD3-FITC (145-2C11), anti-CD8-PerCPCy5.5 (53-6.7), anti-CD4-APC (RM4-5), anti-CD62L-PE (MEL-14), and anti-CD44-Alexa Fluor<sup>®</sup> 700 (IM7) (all from BD Biosciences) were then used for cell-surface staining.

Purified CD8<sup>+</sup> and CD4<sup>+</sup> T cells were isolated from splenocytes of wild-type and THY-Tau22 mice by magnetic cell sorting, using Dynal Mouse CD4 negative isolation kit and Dynabeads<sup>®</sup> untouched mouse CD8 cells kit (Invitrogen), according to manufacturer's instructions. Purity of isolated cells was evaluated by flow cytometry using anti-CD3-FITC (145-2C11), anti-CD8-PerCPCy5.5 (53-6.7), anti-CD4-APC (RM4-5), anti-CD19-PE (1D3) (all from BD Biosciences). Purity of isolated CD8<sup>+</sup> and CD4<sup>+</sup> T cells was >80%.

For the analysis of activation-induced cytokine production,  $2 \times 10^6$  splenocytes from wild-type or THY-Tau22 mice were stimulated *in vitro* for 5 h at 37°C with a cocktail of PMA + ionomycin (Leukocyte Activation Cocktail; BD Biosciences) in the presence of brefeldin A. Cells were then harvested, incubated with FcR-blocking antibody (2.4G2) to avoid non-specific staining, and surface-stained using anti-CD3-FITC (145-2C11), anti-CD8-PerCPCy5.5 (53-6.7), anti-CD4-APC-eFluor780 (GK1.5; eBioscience). After cell surface staining cells were processed for intracellular cytokine staining using the BD Cytofix/Cytoperm kit (BD Biosciences). After permeabilization, cells were first incubated with FcR-blocking antibody (2.4G2), followed by anti-IFN $\gamma$ -PE-Cy7 (XMG1.2;

BD Biosciences) and anti-TNF $\alpha$ -BV421 (MP6-XT22; Biologend).

All fluorescence data related to T cell analyses were collected on a Gallios flow cytometer (Beckman Coulter) and analysed using Kaluza Analysis 1.3 software (Beckman Coulter).

## Statistical analysis

Results are expressed as means  $\pm$  SEM or  $\pm$  standard deviation (SD). Differences between mean values were determined using the Student's *t*-test or one-way ANOVA followed by a *post hoc* Fisher's least significant difference (LSD) test using Graphpad Prism Software. *P* values < 0.05 were considered significant.

## Results

### Development of hippocampal neuroinflammation in THY-Tau22 mice

We first evaluated glial cell activation in the hippocampus of THY-Tau22 mice, from an early stage (3 months of age), *i.e.* when hippocampal tau pathology starts developing, to later stages (12 months of age), when pathology and memory deficits are maximal in this mouse model (Burnouf *et al.*, 2012; Van der Jeugd *et al.*, 2013). As expected from previous studies in several tau transgenic models (Yoshiyama *et al.*, 2007; Bellucci *et al.*, 2011; Laurent *et al.*, 2014), immunostainings for CD11b and GFAP showed significant microgliosis and astrocytosis, which were spatiotemporally correlated with hippocampal tau pathology in THY-Tau22 mice, as compared to wild-type littermates (Fig. 1). Accordingly, we found significant mRNA upregulation of innate immunity markers such as *Tlr2* (toll-like receptor 2), *Cd68* and *Tnfa* (tumor necrosis factor  $\alpha$ ) (Supplementary Fig. 1).

To gain further insights into the relationships between tau pathology and neuroinflammation, we performed a microarray study on hippocampal mRNA samples from 12 month-old wild-type and THY-Tau22 mice ( $n = 7/$  group), to evaluate global gene expression changes associated with the development of tauopathy. As shown in Supplementary Table 2, 32 genes were identified as differentially expressed, with 28 genes being upregulated and only four genes downregulated in THY-Tau22 mice, as compared to wild-type animals. Most of the upregulated genes were associated with immune responses, in line with GO-Term Enrichment analysis (Supplementary Table 2). Expression changes of uncovered immune markers (indicated as bold in the Supplementary Table 2) were validated by quantitative PCR using independent mRNA samples. For most markers, such analysis demonstrated an age-dependent increased expression in tau transgenic mice as compared to wild-type littermates (Fig. 2A and Supplementary Fig. 2). Altogether, these data indicate that significant neuroinflammatory responses progressively

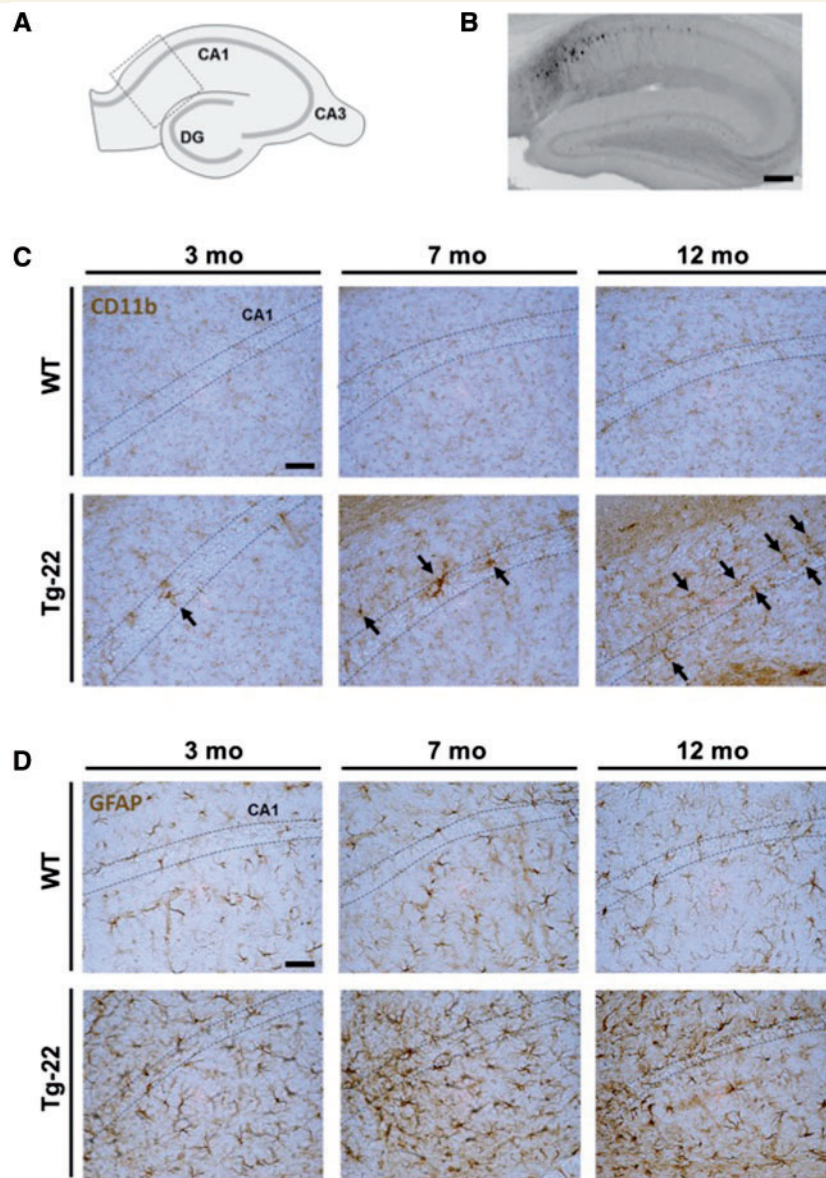


**Figure 1** Glial cell activation in the hippocampus of THY-Tau22 mice. (A and B) As seen using an antibody revealing pSer422 immunoreactivity, THY-Tau22 mice exhibit a high level of abnormally phosphorylated tau species in the CA1 region of hippocampus at 12 months of age. (C and D) CD11b immunostaining point out progressive microglial (C, arrows) and astroglial (D) responses in the hippocampal CA1 area of THY-Tau22 mice (bottom) as compared to wild-type (WT) animals (top).  $n = 3/\text{group}$ . Scale bars = 500  $\mu\text{m}$  (B); 100  $\mu\text{m}$  (C and D).

develop along with tau pathology and memory deficits in the hippocampus of THY-Tau22 mice.

### Chemokine surge is associated with hippocampal T cell infiltration

Among the 28 genes overexpressed in the hippocampus of THY-Tau22 mice (Supplementary Table 2), four of them encode chemokines, i.e. *Ccl3*, *Ccl4*, *Ccl5* and *Cxcl5*. Upregulation of CCL3, CCL4 and CCL5 was confirmed by both quantitative PCR and ELISA (Fig. 2A and B). Of note, compared to CCL4 and CCL5, hippocampal CCL3

levels were progressively and significantly upregulated from early pathological stages as compared to control littermates (Fig. 2B). Immunofluorescence analysis revealed clustered CCL3 staining in Iba1-positive (Fig. 2C) but not GFAP-positive (Fig. 2C) hippocampal cells, suggesting that CCL3 is almost exclusively produced by microglia in the hippocampus of THY-Tau22 mice.

Chemokines are pivotal in the trafficking of leucocytes into the brain (Jaerve and Müller, 2012). Among them, CCL3 was suggested to favour T cell infiltration in the brain of patients with Alzheimer's disease (Man *et al.*, 2007). To test the hypothesis that chemokine release in the hippocampus of THY-Tau22 mice was associated

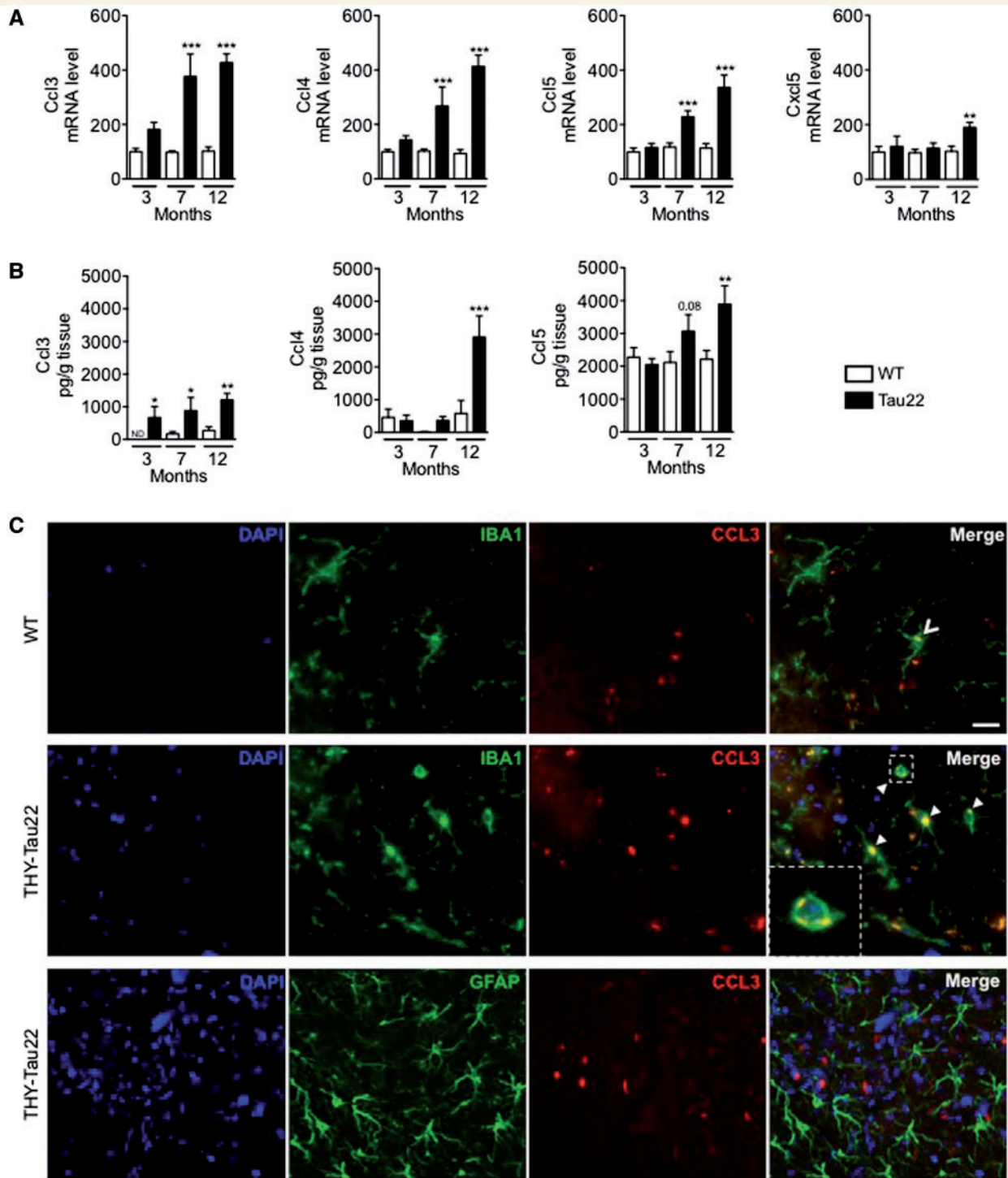


**Figure 2** Age-dependent upsurge of chemokines in the hippocampus of THY-Tau22 mice. **(A)** Quantitative PCR analysis of *Ccl3*, *Ccl4*, *Ccl5* and *Cxcl5* mRNAs revealed a significant and generally progressive overexpression in the hippocampus of transgenic animals as compared to wild-type (WT). Results are expressed as means  $\pm$  SEM. \* $P < 0.05$ , \*\* $P < 0.01$ , \*\*\* $P < 0.001$  versus wild-type (3 months) using one-way ANOVA followed by a *post hoc* Fisher's LSD test.  $n = 5$ –13/group. **(B)** ELISA determinations of hippocampal CCL3, CCL4 and CCL5 levels in wild-type and THY-Tau22 mice at all ages. The three chemokines were found significantly increased in tau animals, CCL3 being the earliest upregulated chemokine. Results are expressed as means  $\pm$  SEM. \* $P < 0.05$ , \*\* $P < 0.01$ , \*\*\* $P < 0.001$  versus wild-type (3 months) using one-way ANOVA followed by a *post hoc* Fisher's LSD test.  $n = 6$ –8/group. **(C)** Immunofluorescence analysis of CCL3 expression in the hippocampus of THY-Tau22 mice and wild-type littermates at the age of 12 months. Labelling of CCL3 (red) with the microglial marker Iba1 or the astrocyte marker GFAP (green) revealed clustered CCL3 staining solely in Iba1-positive cells (arrowheads and inset) in transgenic tau mice. To a lesser extent, such clusters are present in wild-type animals. Scale bar = 20  $\mu$ m.

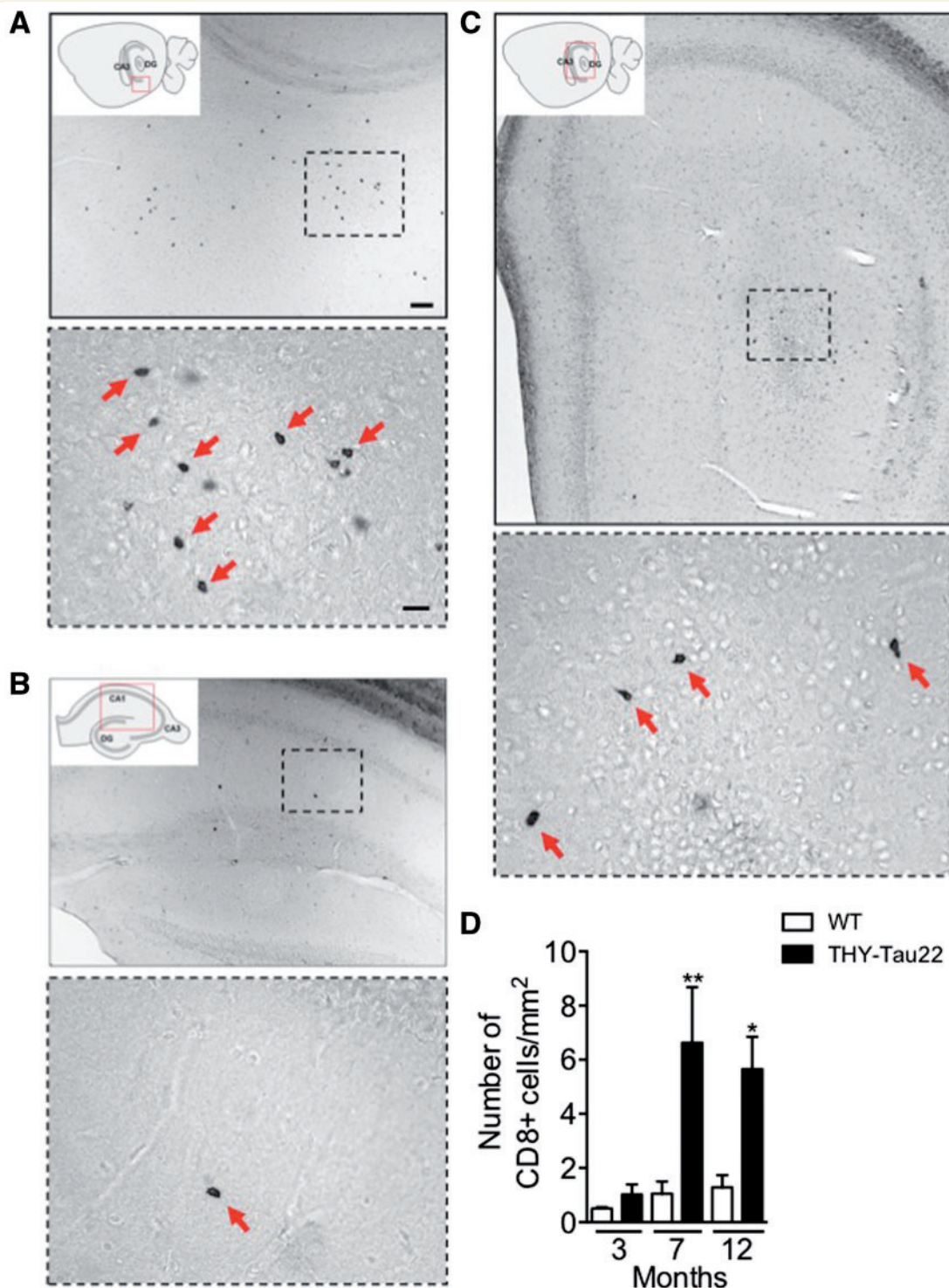


**Figure 3 Hippocampal CD8<sup>+</sup> T cell infiltration in the parenchyma of THY-Tau22 mice.** (A–C) *Top*: CD8 immunostaining highlights numerous parenchymal lymphocytes in the whole hippocampus of tau transgenic animals. Infiltrated lymphocytes were clearly identified at higher magnification (red arrows in *bottom* panels). (D) Hippocampal density of CD8<sup>+</sup> T cells was found significantly increased from 7 months of age. Results are expressed as means  $\pm$  SEM. \* $P < 0.05$ , \*\* $P < 0.01$  versus wild-type mice using one-way ANOVA followed by a *post hoc* Fisher's LSD test.  $n = 3$ /group.

with T cell recruitment, hippocampal CD4<sup>+</sup> and CD8<sup>+</sup> T cells were quantified by immunohistochemistry. Numerous CD8<sup>+</sup> cells exhibiting typical lymphocyte morphology

accumulated in the hippocampus of THY-Tau22 mice all along the rostro-caudal axis, an area exhibiting hyperphosphorylated tau species (Fig. 3A–C). Quantitative

analysis revealed a significant increase in the density of hippocampal CD8<sup>+</sup> T cells in THY-Tau22 mice as compared to wild-type animals, starting from 7 months of age (Fig. 3D). Unlike CD8<sup>+</sup> T cells, parenchymal CD4<sup>+</sup> cells were barely observed in both THY-Tau22 mice and wild-type littermates at all ages (not shown). As chemokines, and notably CCL3, can also be a chemoattractant for myeloid cells (Trifilo *et al.*, 2003), we have also determined by flow cytometry the proportion of microglia (CD11b<sup>+</sup>CD45<sup>med</sup>) and peripheral macrophages (CD11b<sup>+</sup>CD45<sup>high</sup>) in the brain of THY-Tau22 mice. We found that the proportion of macrophages was not increased in the brain of THY-Tau22 mice compared to wild-type mice at the age of 6 and 12 months, indicating that macrophages do not significantly infiltrate the CNS during the pathology (Supplementary Fig. 3).

In parallel, we also evaluated the activation status of peripheral T cells in THY-Tau22 mice. We carried out a detailed phenotypic analysis of both CD8<sup>+</sup> and CD4<sup>+</sup> T cells in the blood, spleen and pooled lymph nodes (cervical, axillary and inguinal) from 5/6-months old wild-type and THY-Tau22 mice, based on the expression of CD44 and CD62L activation markers. We observed no differences in the frequency of naive (CD62L<sup>+</sup>CD44<sup>low</sup>), effector memory (CD62L<sup>-</sup>CD44<sup>hi</sup>), central memory (CD62L<sup>+</sup>CD44<sup>hi</sup>) or acute/activated effector (CD62L<sup>-</sup>CD44<sup>low</sup>) CD8<sup>+</sup> or CD4<sup>+</sup> T cells (Supplementary Fig. 4). Hence, human tau transgene expression in THY-Tau22 mice did not result in altered balance of activated versus naive CD8<sup>+</sup> nor CD4<sup>+</sup> T cells in the periphery. Furthermore, to rule out a potentially altered functionality of peripheral T cells in THY-Tau22 mice due to potential transgene expression in CD4<sup>+</sup> and/or CD8<sup>+</sup> T cells, we analysed the expression of human *MAPT* (tau) transgene in purified CD4<sup>+</sup> and CD8<sup>+</sup> T cells isolated from the spleens of both wild-type and tau transgenic mice. As expected from previous works showing that the Thy1.2 expression cassette only drives expression solely in neurons and not T cells (Vidal *et al.*, 1990; Caroni, 1997), we did not detect any human 4R tau transgene in both purified CD4<sup>+</sup> and CD8<sup>+</sup> T cells from THY-Tau22 mice (Supplementary Fig. 5). Finally, we assessed whether peripheral T cells from transgenic mice may display any altered functionality at producing effector cytokines as compared to T cells from wild-type mice. By intracellular cytokine staining and flow cytometry analysis, we quantified the frequency of CD4<sup>+</sup> and CD8<sup>+</sup> T cells producing key effector cytokines interferon- $\gamma$  (IFN $\gamma$ ) and/or TNF $\alpha$  upon polyclonal activation of either wild-type or THY-Tau22 splenocytes. No significant differences were observed in the frequency of TNF $\alpha$ -producing CD8<sup>+</sup> T cells, as well as in percentages of IFN $\gamma$ <sup>+</sup>TNF $\alpha$ <sup>-</sup> or IFN $\gamma$ <sup>+</sup>TNF $\alpha$ <sup>+</sup> CD4<sup>+</sup> T cells, between wild-type and transgenic animals (Supplementary Fig. 6). These data indicate that 4RTau transgene is neither significantly expressed at the protein level in CD4<sup>+</sup> and CD8<sup>+</sup> T cells from THY-Tau22 animals, nor does it impair their capacity to produce effector cytokines upon activation. Altogether, these studies

rule out a possible impact of human tau transgene expression in T cells on their activation profile and functionality in THY-Tau22 mice. Hence, these data further suggest that hippocampal T cell infiltration in THY-Tau22 animals is not a bystander effect resulting from potentially altered functionality of peripheral T cells prior entering the brain, but rather related to brain-restricted neuroinflammatory processes triggering selective CD8<sup>+</sup> T cell recruitment.

To confront the data obtained in our experimental model of tauopathy-associated cognitive impairment with human pathology, we investigated CD8<sup>+</sup> T cell recruitment in post-mortem brain specimens from patients exhibiting frontotemporal dementia with tau P301L mutations and age-matched control individuals. As expected, tau hyperphosphorylation was observed in the cortex of patients with frontotemporal dementia carrying P301L mutations (Fig. 4A). Whereas CD8<sup>+</sup> T cells were exclusively distributed along the blood vessels in control individuals, both vascular and parenchymal CD8<sup>+</sup> cells were systematically observed in patients suggesting that tau pathology is associated with brain tissue recruitment and infiltration of CD8<sup>+</sup> T cells at distance from the blood–brain barrier (Fig. 4B).

As T cell entry could rely on passive mechanisms due to blood–brain barrier breakdown (Blair *et al.*, 2015), we evaluated the integrity of the blood–brain barrier by analysing the status of tight junctions and the potential presence of IgG extravasation in the hippocampus of THY-Tau22 mice. Immunostainings show a similar overlap for tight-junctions markers zonula occludens-1 and occludin, with the constitutive endothelial marker von Willebrand factor in the hippocampus of 12-month-old THY-Tau22 mice as compared to wild-type animals (Fig. 5 and Supplementary Fig. 7). *Tjp1* (zonula occludens-1) and *Ocln* (occludin) mRNA expressions also remained unchanged (not shown). Finally, we did not find any sign of IgG extravasation in THY-Tau22 mice, supporting the lack of major blood–brain barrier disruption (Supplementary Fig. 8). Altogether our data support that hippocampal tau pathology is sufficient for promoting active brain-restricted recruitment of CD8<sup>+</sup> T cells.

## T cell depletion restrains cognitive deficits in THY-Tau22 mice

To evaluate the impact of T cell infiltration on disease progression, we assessed the consequences of T cell depletion on pathophysiological development in THY-Tau22 mice. Tau transgenic animals were injected every 2 weeks with either anti-CD3 depleting antibody or control isotype from 4 to 9 months of age, i.e. starting from an early disease stage before T cell infiltration can be detected up to later stages when hippocampal T cell accumulation is maximal (Fig. 3B). As shown in Supplementary Fig. 5, TCR $\beta$ <sup>+</sup> circulating T cells drop dramatically 5 days after anti-CD3 treatment as compared to isotype-treated mice, while

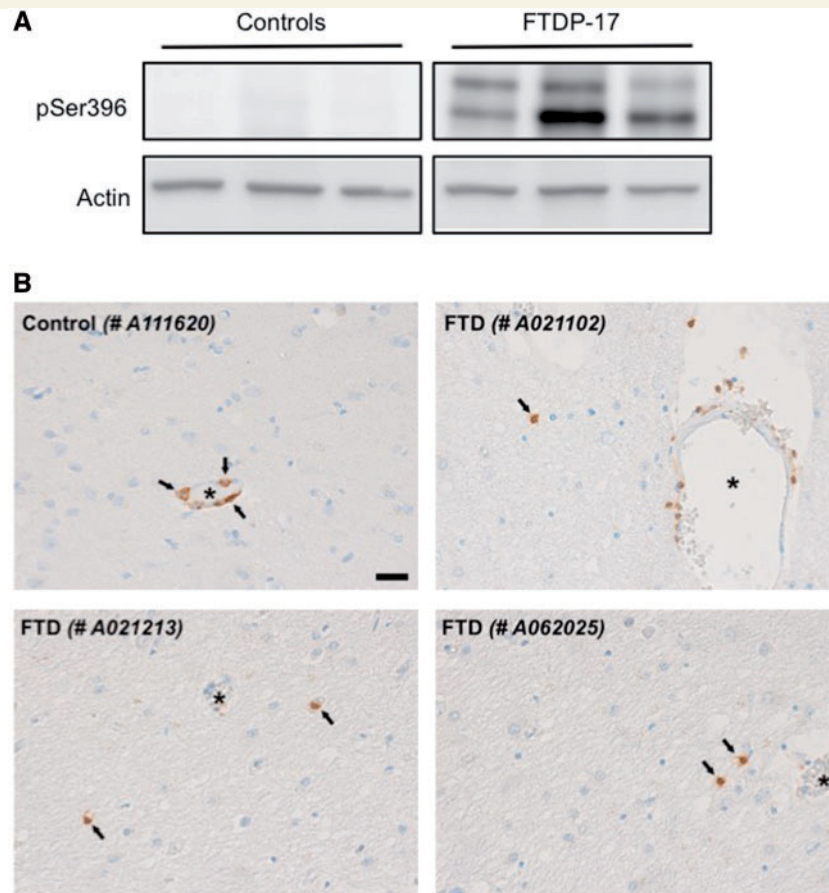


**Figure 4** Presence of parenchymal CD8<sup>+</sup> cells in the cortex of patients with frontotemporal dementia (FTDP-17) carrying P301L mutations. (A) Western blot analysis performed on the cortex of patients revealed, as expected, tau hyperphosphorylation at pSer396 epitope as compared to age-matched controls ( $n = 3/\text{group}$ ). (B) Immunohistochemical detection of CD8<sup>+</sup> T cells in the human cortex of controls and patients. Whereas CD8<sup>+</sup> T cells were exclusively distributed along the blood vessels (indicated by an asterisk) in control individuals, parenchymal (arrows) CD8<sup>+</sup> cells are observed at distance from the blood–brain barrier in patients. Scale bar = 100  $\mu\text{m}$ .

CD19<sup>+</sup> B cells remain unchanged. Drastic decrease in both frequency and absolute numbers of TCR $\beta$ <sup>+</sup> T cells but not B cells was also observed in spleen and pooled lymph nodes, confirming the efficiency and specificity of T cell depletion approach (Supplementary Fig. 9C and D). On completion of treatment, i.e. in 9-month-old animals, we examined the impact of T cell depletion on the development of memory deficits in THY-Tau22 mice, using the Y-maze task.

Treatment of wild-type littermates with either anti-CD3 or control isotype did not significantly impact spatial memory. Indeed, as shown in Fig. 6A, wild-type animals spent significantly more time in the novel arm as compared to the other one ( $P < 0.001$  versus other arm for both groups; one-way ANOVA). Accordingly, percentage of time spent in the novel arm was significantly above chance (i.e. >50%) in both groups (wild-type + isotype:  $P = 0.01$ ; wild-type + anti-CD3:  $P = 0.027$ ). As expected (Belarbi *et al.*, 2011; Laurent *et al.*, 2016), THY-Tau22 mice injected with control isotype exhibited impaired spatial memory as demonstrated by the lack of preference for

the novel arm ( $P = 0.69$  when compared to 50% chance, and  $P = 0.61$  versus the other arm; one-way ANOVA). In contrast, THY-Tau22 animals treated with anti-CD3 antibody behaved like wild-type animals, spending significantly more time in the novel arm than the other arm ( $P = 0.011$  when compared to 50% chance,  $P < 0.0001$  versus other arm; one-way ANOVA), indicative of improved spatial memory upon T cell depletion (Fig. 6A). Impaired memory has been associated with altered plasticity in tau transgenic mice (Burlot *et al.*, 2015). We then investigated to what extent anti-CD3 treatment impacted on markers known to modulate synaptic plasticity. Specifically, we studied expression of Arc and 14-3-3 proteins, both known to regulate hippocampal-dependent memory (Qiao *et al.*, 2014; Minatohara *et al.*, 2016). As shown in Fig. 6B, hippocampal expression of Arc and 14-3-3 significantly decreased, respectively, by  $42.9 \pm 1.9\%$  ( $P = 0.016$ ) and  $23.0 \pm 0.9\%$  ( $P = 0.014$ ) in THY-Tau22 injected with isotype compared to wild-type mice treated with isotype. Whereas anti-CD3 antibody did not impact on Arc and 14-3-3 expressions in wild-type mice, their levels were

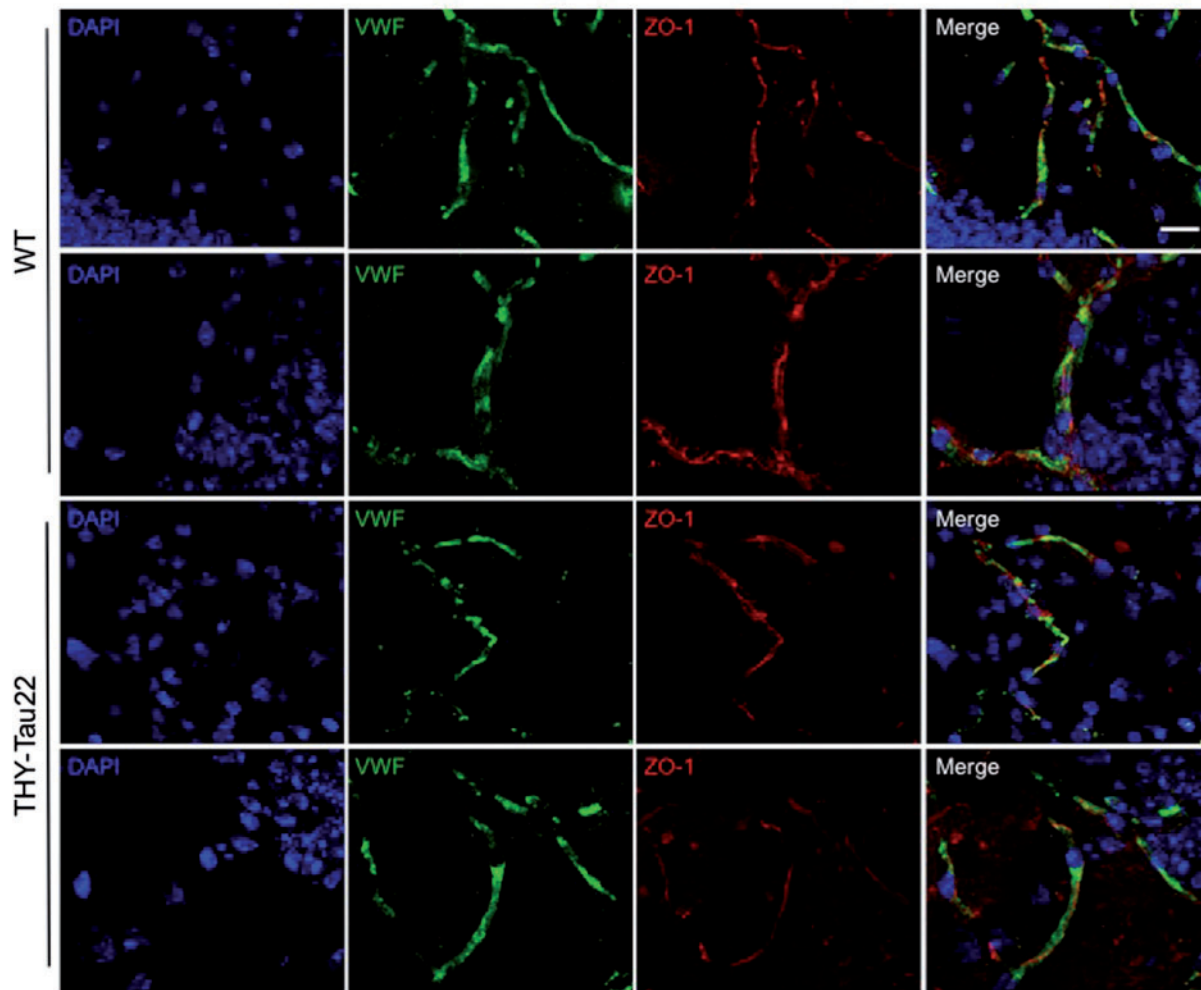


**Figure 5 Blood–brain barrier integrity of THY-Tau22 mice.** Immunofluorescence labelling of the tight junction marker zonula occludens-1 (ZO-1; red) and the constitutive endothelial marker von Willebrand factor (VWF; green) in the CA1 region of the hippocampus of wild-type (WT; *top*) and THY-Tau22 mice (*bottom*) at 12 months of age. DAPI staining of nuclei in blue. Similar co-stainings was observed in both genotypes, reflecting an absence of major blood–brain barrier impairment in transgenic animals.  $n = 3/\text{group}$ . Scale bar = 20  $\mu\text{m}$ .

significantly increased in THY-Tau22 mice treated with the antibody (Arc:  $+32.2 \pm 6.7\%$ ,  $P = 0.025$  versus THY-Tau22 + isotype; 14-3-3:  $25.6 \pm 7.6\%$ ,  $P = 0.023$  versus THY-Tau22 + isotype, one-way ANOVA; Fig. 6B). Strikingly, prevention of spatial memory deficits was associated with a significant reduction in the density of CD8<sup>+</sup> cells in the hippocampus of T-cell-depleted THY-Tau22 mice, reaching similar levels than in control littermates (Fig. 6C).

We demonstrated previously a correlation between spatial memory impairment and tau hyperphosphorylation in the THY-Tau22 mouse model (Burnouf *et al.*, 2013; Leboucher *et al.*, 2013; Laurent *et al.*, 2016). We thus investigated the impact of T cell depletion on hippocampal tau phosphorylation in THY-Tau22 mice. Immunohistochemical studies showed that percentage of AT8-stained hippocampal area was similar in both groups of THY-Tau22 mice ( $1.13 \pm 0.11\%$  in isotype-treated mice versus  $1.39 \pm 0.22\%$  after anti-CD3 treatment;  $P > 0.05$ ,

Student *t*-test; Fig. 6D). Western blot experiments further indicated that T cell depletion did not alter tau expression, truncation or phosphorylation at multiple epitopes (Fig. 6E). Of note, quantitative RT-PCR analysis showed that T cell depletion was associated with significant reduction of *Clec7a*, *Itgax*, *Ccl3*, *Cd52*, *Gfap* and *Cd68* mRNA expression levels in THY-Tau22 mice as compared to isotype-treated transgenic animals (Fig. 6F). Altogether, these data strongly support that hippocampal CD8<sup>+</sup> T cell infiltration promotes neuroinflammation and cognitive decline in THY-Tau22 transgenic mouse model of tauopathy, without affecting tau protein deposition or phosphorylation.

## Discussion

Accumulating evidence support an instrumental role of immunity in the pathophysiology of Alzheimer's disease.

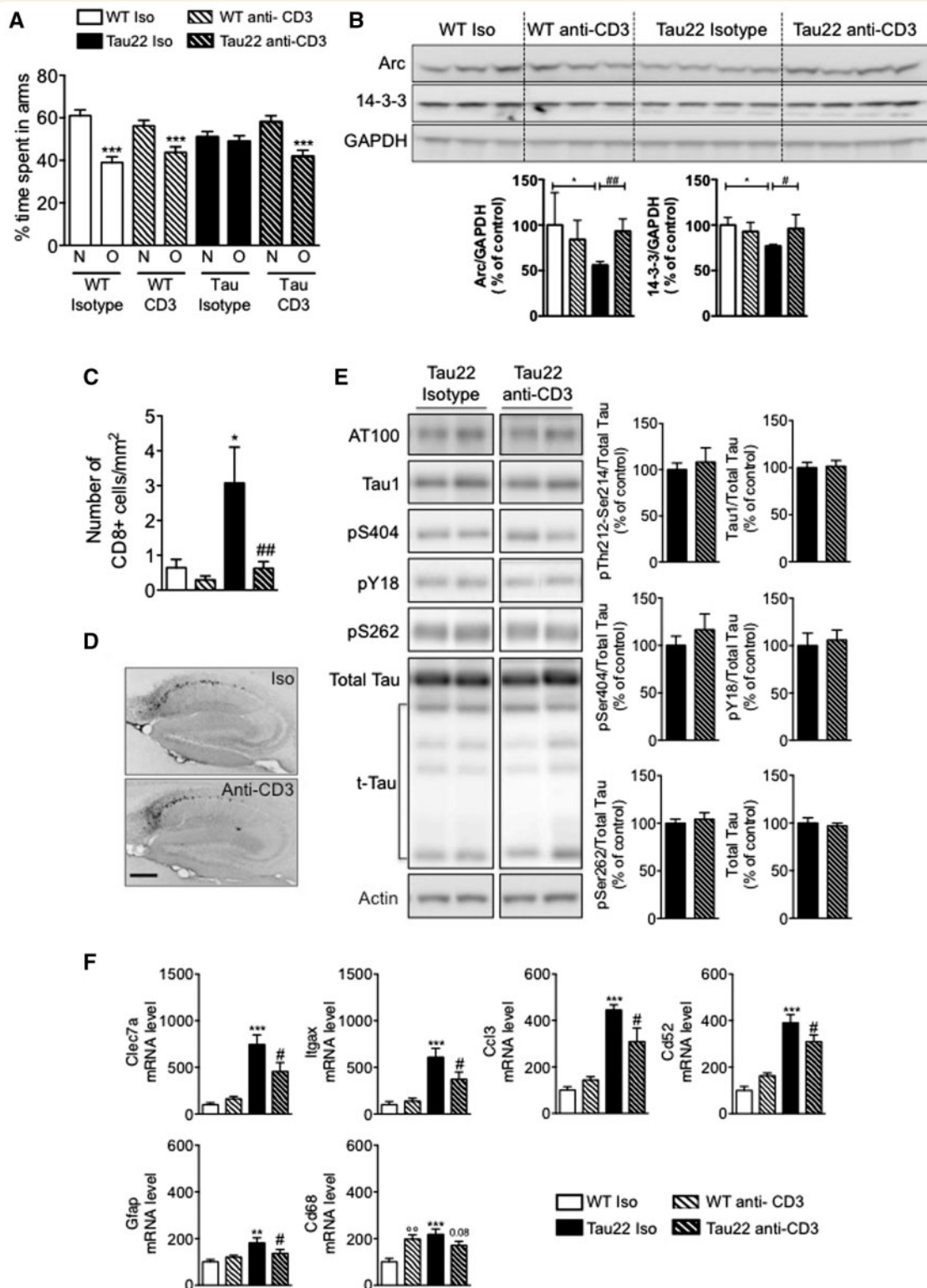


**Figure 6** Impact of T cell depletion on spatial memory and hippocampal tau pathology in THY-Tau22 mice. (A) Effect of anti-CD3 antibody treatment on spatial memory using Y-maze task. While wild-type (WT) mice, regardless of treatment, exhibited a preference for the new arm, compared to the familiar arm, THY-Tau22 treated with the isotypic control did not demonstrate preference for the new arm, showing defective spatial memory. By contrast, anti-CD3 treated THY-Tau22 mice demonstrated a preference for the new arm similarly to control animals. Results are expressed as means  $\pm$  SEM. \*\*\* $P$  < 0.001 Familiar/Other (O) versus New (N) arms using one-way ANOVA.  $n$  = 6–19/group. (B) Effect of T cell depletion on hippocampal markers of synaptic plasticity. Hippocampal Arc and 14-3-3 immunoreactivities were found significantly decreased in THY-Tau22 mice treated with isotypic control versus wild-type mice and return to control level in THY-Tau22 mice treated with the anti-CD3 antibody. \* $P$  < 0.05, versus wild-type isotype, # $P$  < 0.05 and ### $P$  < 0.01 versus THY-Tau22 isotype group, using

(continued)

Whereas most previous studies focused on amyloid-driven pathology, interrelationships between innate and adaptive immune responses with tau pathology remain unclear so far. Our study in a tau transgenic mouse model highlights that tau pathology is associated with an early chemokine surge followed by hippocampal T cell infiltration. Importantly, our data support that such T cell recruitment promotes tau-triggered spatial memory deficits, without affecting tau protein deposition nor phosphorylation, but at least partially through promoting innate neuroinflammatory responses. To the best of our knowledge, this is the first report documenting an instrumental role of brain T cell infiltration in the pathophysiology of tauopathy.

In the present work, we describe that development of hippocampal tauopathy, previously linked to significant cognitive deficits (Van der Jeugd *et al.*, 2011; Burnouf *et al.*, 2013; Laurent *et al.*, 2016), induces progressive innate neuroinflammatory response associated with T cell recruitment in the absence of neuronal death (Van der Jeugd *et al.*, 2011; Burnouf *et al.*, 2013). Innate neuroinflammation has previously been associated with tau pathology (Yoshiyama *et al.*, 2007; Garwood *et al.*, 2010) and is thought to contribute, in a vicious circle, to tau hyperphosphorylation, aggregation, secretion and pathology spreading (Yoshiyama *et al.*, 2007; Gorlovoy *et al.*, 2009; Bhaskar *et al.*, 2010; Asai *et al.*, 2015). Microglia activation can result in multiple phenotypes characterized by distinct molecular and functional patterns. In particular, classical proinflammatory M1-like phenotype, such as induced by the prototypic activation cocktail Lipopolysaccharide plus IFN $\gamma$ , is associated with expression of proinflammatory mediators (TNF $\alpha$ , interleukin 1 $\beta$ , interleukin 6, ...) as well as several chemokines including CCL3 (for review see Mantovani *et al.*, 2004). Here, we demonstrate that development of tau pathology is associated with an early and progressive surge of microglial-produced CCL3 in the hippocampus of THY-Tau22 mice. Together with TNF $\alpha$  expression observed at later stages, these data suggest that tau-associated microglial activation in our transgenic mice is reminiscent of a proinflammatory-like profile. Early increase in Toll-like receptor 2 expression further supports this idea, as Toll-like receptor 2 expression is associated with M1-like microglial polarization profile and function (Liu *et al.*, 2012). Hippocampal CCL3 upregulation in THY-Tau22 mice could contribute to several mechanisms converging to memory deficits. As we

previously demonstrated in wild-type mice (Marciniak *et al.*, 2015), CCL3 could directly alter long-term plasticity and spatial memory in the hippocampus of THY-Tau22 mice. In addition, our current data support that tau-triggered CD8<sup>+</sup> T cell infiltration in the brain contributes to the development of memory impairments. Interestingly, CCL3 production is detected before T cell infiltration and could therefore contribute to T cell diapedesis. Indeed, among other chemokines, CCL3 has been shown to contribute to T cell recruitment to the brain (Man *et al.*, 2007; Shechter *et al.*, 2013; see Wilson *et al.*, 2010 for review). Leucocyte infiltration has been recently reported in tau transgenic animals (Blair *et al.*, 2015). However, in this study using the rTg4510 strain, infiltration of CD3<sup>+</sup> cell was strongly associated with tau-induced neurotoxicity and blood–brain barrier damage, as notably seen using IgG staining. Our data rather suggest that development of tau pathology is associated with T cell hippocampal recruitment that occurs in the absence of major blood–brain barrier leakage, in favour of an active process possibly involving CCL3-mediated chemotaxis. This view is further supported by increased *Itgb2* (lymphocyte function-associated antigen 1/LFA-1), *Vcam1* (vascular cell adhesion molecule 1), and *Icam1* (intercellular adhesion molecule) mRNA expression in the hippocampus of THY-Tau22 mice (not shown). It is worth noting that T cell infiltration was neither related to an altered T cell activation profile nor impaired functionality in the periphery prior to entering the brain, ruling out that our observations rely on skewed functional differentiation of T cells in our transgenic mouse model. Lymphocyte infiltration has been described in brains of patients with Alzheimer's disease (Rogers *et al.*, 1988; Togo *et al.*, 2002; Zotova *et al.*, 2013), as well as in murine models of amyloid-driven pathology (Stalder *et al.*, 2005; Browne *et al.*, 2013). Of note, Zotova *et al.* (2013) pointed out that presence of CD3<sup>+</sup> T cells in the brain parenchyma of patients correlated with phospho-tau but not amyloid pathology. In the present manuscript, we qualitatively observed parenchymal CD8<sup>+</sup> cells in the cortex of patients exhibiting frontotemporal dementia carrying P301L tau mutation, in accordance with CD8<sup>+</sup> cell infiltration evidenced in THY-Tau22 mice. Altogether, these data support that tau-triggered innate neuroinflammatory responses may promote CD8<sup>+</sup> T cell infiltration into the brain of patients with Alzheimer's disease. Of note, antigen specificity of such infiltrating T cells

#### Figure 6 Continued

one-way ANOVA followed by a *post hoc* Fisher's LSD test.  $n = 3\text{--}4/\text{group}$ . Hippocampal density of CD8<sup>+</sup> T cells in the different experimental groups. Density of CD8<sup>+</sup> T cells was significantly increased at 9 months of age in THY-Tau22 mice treated with isotype and returned to control level in THY-Tau22 mice treated with anti-CD3 antibody. \* $P < 0.05$  versus wild-type isotype, ### $P < 0.01$  versus THY-Tau22 isotype group, using one-way ANOVA followed by a *post hoc* Fisher's LSD test.  $n = 3\text{--}10/\text{group}$ . (D) AT8 immunostaining indicate a similar immunoreactivity in THY-Tau22 mice regardless of treatment.  $n = 8/\text{group}$ . Scale bar = 500  $\mu\text{m}$ . (E) Anti-CD3 treatment did not impact human tau expression, truncation (t-tau) and hyper-phosphorylation at several phospho-epitopes in THY-Tau22 mice.  $n = 6\text{--}8/\text{group}$ . Results are expressed as a percentage of THY-Tau22 mice injected with isotype  $\pm$  SEM. (F) Effect of anti-CD3 treatment upon mRNA expression of neuroinflammatory markers in the hippocampus of THY-Tau22 mice. \*\* $P < 0.01$ , \*\*\* $P < 0.001$  versus wild-type isotype, # $P < 0.05$  versus THY-Tau22 isotype group, using one-way ANOVA followed by a *post hoc* Fisher's LSD test.  $n = 6\text{--}9/\text{group}$ .

still remains unknown, as well as whether their selective hippocampal recruitment relies on antigen-specific transmigration processes, as previously described in murine models of multiple sclerosis (Galea *et al.*, 2007).

Our study supports that tau-triggered T cell infiltration plays an instrumental role in the development of tau-induced memory deficits. Whereas anti-CD3 treatment had no significant effect in wild-type littermates, such peripheral T cell depletion in THY-Tau22 mice abolished both CD8<sup>+</sup> T cell infiltration in the hippocampus and cognitive deficits, as measured using the short-term memory Y-maze task, previously shown to be very sensitive in the THY-Tau22 strain (Belarbi *et al.*, 2011; Troquier *et al.*, 2012; Burlot *et al.*, 2015; Laurent *et al.*, 2016). Noteworthy, behavioural improvement occurred without detectable impact on tau phosphorylation nor deposition, suggesting that T cell infiltration is not instrumentally involved in the direct modulation of tau proteinopathy, but rather stands as a downstream factor promoting cognitive impairment. In accordance with this view, we observed that tau-pathology induced downregulation of Arc and 14-3-3 proteins, both involved in hippocampal synaptic plasticity and the formation of memory traces (Qiao *et al.*, 2014; Minatohara *et al.*, 2016), which was prevented by anti-CD3 treatment in THY-Tau22 mice. Of note, our data show that T cell depletion was associated with significant downregulation of several neuroinflammatory markers in THY-Tau22 mice, suggesting differential activation of astrocytic and microglial responses in T cell-depleted animals. Activated microglia and astrocytes can produce a significant range of soluble factors capable of modulating synaptic function and plasticity, such as inflammatory mediators, trophic factors, neurotransmitters and neuromodulators. Variations in the activation phenotypes of such glial cell populations is expected to translate into different capacities to modulate cognitive functions (Jones and Lynch, 2015; Patterson, 2015). Hence, hippocampal T cells infiltrating the brain in the context of tau pathology may directly modulate microglial and/or astrocytic activation status, towards a profile with detrimental impact on synaptic plasticity. This is in part reminiscent of our recent data in a mouse model of amyloid-driven pathology, suggesting that some T cell populations, i.e. regulatory T cells, inversely contribute to restrain cognitive deficits at least partially through modulation of microglial responses, without altering amyloid- $\beta$  deposition (Dansokho *et al.*, 2016). Of note, it was recently suggested that the complement-dependent pathway of synaptic pruning by microglia is inappropriately activated and mediate synapse loss in Alzheimer's disease (Hong *et al.*, 2016). Considering that complement has previously been described to contribute to the regulation of T cell functional differentiation, expansion and survival (Kwan *et al.*, 2012), it now remains to be determined whether the impact of complement pathway on synapse loss may also partly rely on complement-mediated regulation of T cell responses and/or their crosstalk with microglia.

Alternatively, hippocampal CD8<sup>+</sup> T cells might also directly affect neuronal function and plasticity. Several evidence

indicates that neurons can express major histocompatibility complex class I molecules, either constitutively or more particularly in an inflammatory context. Both antigen-dependent and antigen-independent interactions between neurons and T cells, including CD8<sup>+</sup> T cells, have been previously described. Among other mechanisms, based on antigen- and major histocompatibility complex class I-dependent interactions, CD8<sup>+</sup> T cells were shown to promote direct localized structural damage to neurites, or even neuron lysis (Pool *et al.*, 2012; Sauer *et al.*, 2013). Activated CD8<sup>+</sup> T cells can also inhibit neurite outgrowth without detectable neuronal apoptosis in a contact-dependent but antigen-independent manner (reviewed in Liblau *et al.*, 2013). Cytokines released from activated T cells might also contribute to direct and collateral disturbances of neuronal electrical activity. Further investigations will be needed to determine whether such mechanisms occur in the context of tau pathology.

A recent report in mouse models of amyloid pathology suggested that boosting overall T cell responses via immune checkpoint blockade reduces pathology and improves memory, supporting a beneficial role for CNS-specific cell-mediated immunity in Alzheimer's disease and potentially other neurodegenerative disorders (Baruch *et al.*, 2016). Whereas our previous studies in a mouse model of Alzheimer's disease-like amyloid pathology suggested that amyloid- $\beta$ -specific CD8<sup>+</sup> T cells do not trigger detrimental autoimmune neuroinflammatory processes (Rosset *et al.*, 2015), our current data support a detrimental involvement of proteopathic tau-triggered CD8<sup>+</sup> T cell infiltration in the pathophysiology of Alzheimer's disease and other tauopathies. In addition, using mouse models of amyloid pathology, conflicting results have been reported regarding the impact of regulatory T cells on disease progression, suggesting both beneficial and detrimental impacts, which may vary depending on disease stages (Baruch *et al.*, 2015; Dansokho *et al.*, 2016). Given the unique capacity of regulatory T cells to inhibit T cell responses, our study supporting a pathogenic role of CD8<sup>+</sup> T cells in disease development underlines the need for addressing their role in tau pathology as well.

Our work adds further to the growing body of evidence supporting an instrumental role of cellular adaptive immunity in the pathophysiology of Alzheimer's disease. Importantly, it further highlights the need for better understanding the complex interplay of different T cell populations in the context of both amyloid and tau pathology. Such studies will be required for implementing innovative immunotherapy and/or immunomodulation strategies targeting T cell immunity, which constitute promising approaches for the treatment of Alzheimer's disease.

## Acknowledgements

We express gratitude to patients and their families who allowed us to perform brain autopsies. We are grateful to

the IMPRT (Institut de Médecine Prédictive et de Recherche Thérapeutique, Lille) for access to the confocal microscopy platform and FACS facilities. We thank the animal core facility (animal facilities of Université de Lille–Inserm) of « Plateformes en Biologie Santé de Lille » and M. Besegher, I. Brion, D. Cappe, R. Dehaynin, J. Devassine, Y. Lepage, C. Meunier and D. Taillieu for transgenic mouse production and animal care as well as Meryem Tardivel (imaging facilities of BioImaging center of Lille) for confocal assistance. We also thank Charles Duyckaerts and Claude-Alain Maurage for support.

## Funding

This work was supported by grants from ANR (ADONTAGE, ADORATAU, CYTOKALZ to D.B., P2X7RAD to C.D. and S.S.M., and PARKEMOS to S.H.), Association France Alzheimer, Fondation de France, LECMA/Alzheimer Forschung Initiative, Fondation Plan Alzheimer (to G.D. and D.B.) and from the programs Investissements d'avenir LabEx (excellence laboratory) DISTALZ (Development of Innovative Strategies for a Transdisciplinary approach to Alzheimer's disease), LiCEND excellence centre for neurodegenerative diseases and ANR-10-IAIHU-06. Some of the post mortem samples were collected by the Brain Bank GIE NeuroCEB (BRIF number 0033-00011), funded by the patients' associations France Alzheimer, France Parkinson, ARSEP, 'Connaître les Syndromes Cérébelleux' and by IHU A-ICM and Fondation Plan Alzheimer to which we express our gratitude. Our laboratories are also supported by Inserm, CNRS, Université Lille 2, UPMC, Lille Métropole Communauté Urbaine, Région Nord/Pas-de-Calais, FEDER, DN2M and FUI MEDIALZ. C.L. and A.L. held doctoral grants from Lille 2 University, and S.B. from Région Nord Pas de Calais and CHRU de Lille. E.F. held a post-doctoral grant from Région Nord-Pas-de-Calais (DN2M) and ANR (ADORATAU). The authors declare no conflict of interest regarding the present work.

## Supplementary material

Supplementary material is available at *Brain* online.

## References

- Ahmed T, Blum D, Burnouf S, Demeyer D, Buée-Scherrer V, D'Hooge R, et al. Rescue of impaired late-phase long-term depression in a tau transgenic mouse model. *Neurobiol Aging* 2015; 36: 730–9.
- Asai H, Ikezu S, Tsunoda S, Medalla M, Luebke J, Haydar T, et al. Depletion of microglia and inhibition of exosome synthesis halt tau propagation. *Nat Neurosci* 2015; 18: 1584–93.
- Baruch K, Rosenzweig N, Kertser A, Deczkowska A, Sharif AM, Spinrad A, et al. Breaking immune tolerance by targeting Foxp3(+) regulatory T cells mitigates Alzheimer's disease pathology. *Nat Commun* 2015; 6: 7967.
- Baruch K, Deczkowska A, Rosenzweig N, Tsitsou-Kampeli A, Sharif AM, Matcovitch-Natan O, et al. PD-1 immune checkpoint blockade reduces pathology and improves memory in mouse models of Alzheimer's disease. *Nat Med* 2016; 22: 135–7.
- Belarbi K, Burnouf S, Fernandez-Gomez FJ, Laurent C, Lestavel S, Figeac M, et al. Beneficial effects of exercise in a transgenic mouse model of Alzheimer's disease-like Tau pathology. *Neurobiol Dis* 2011; 43: 486–94.
- Bellucci A, Westwood AJ, Ingram E, Casamenti F, Goedert M, Spillantini MG. Induction of inflammatory mediators and microglial activation in mice transgenic for mutant human P301S tau protein. *Am J Pathol* 2004; 165: 1643–52.
- Bellucci A, Bugiani O, Ghetti B, Spillantini MG. Presence of reactive microglia and neuroinflammatory mediators in a case of frontotemporal dementia with P301S mutation. *Neurodegener Dis* 2011; 8: 221–9.
- Bhaskar K, Konerth M, Kokiko-Cochran ON, Cardona A, Ransohoff RM, Lamb BT. Regulation of tau pathology by the microglial fractalkine receptor. *Neuron* 2010; 68: 19–31.
- Blair LJ, Frauen HD, Zhang B, Nordhues BA, Bijan S, Lin YC, et al. Tau depletion prevents progressive blood-brain barrier damage in a mouse model of tauopathy. *Acta Neuropathol Commun* 2015; 3: 8.
- Braak H, Thal DR, Ghebremedhin E, Del Tredici K. Stages of the pathologic process in Alzheimer disease: age categories from 1 to 100 years. *J Neuropathol Exp Neurol* 2011; 70: 960–9.
- Browne TC, McQuillan K, McManus RM, O'Reilly JA, Mills KH, Lynch MA. IFN- $\gamma$  Production by amyloid  $\beta$ -specific Th1 cells promotes microglial activation and increases plaque burden in a mouse model of Alzheimer's disease. *J Immunol* 2013; 190: 2241–51.
- Burlot MA, Braudeau J, Michaelsen-Preusse K, Potier B, Ayciriex S, Varin J, et al. Cholesterol 24-hydroxylase defect is implicated in memory impairments associated with Alzheimer-like Tau pathology. *Hum Mol Genet* 2015; 24: 5965–76.
- Burnouf S, Belarbi K, Troquier L, Derisbourg M, Demeyer D, Leboucher A, et al. Hippocampal BDNF expression in a tau transgenic mouse model. *Curr Alzheimer Res* 2012; 9: 406–10.
- Burnouf S, Martire A, Derisbourg M, Laurent C, Belarbi K, Leboucher A, et al. NMDA receptor dysfunction contributes to impaired brain-derived neurotrophic factor-induced facilitation of hippocampal synaptic transmission in a Tau transgenic model. *Aging Cell* 2013; 12: 11–23.
- Caroni P. Overexpression of growth-associated proteins in the neurons of adult transgenic mice. *J Neurosci Methods* 1997; 71: 3–9.
- Cao C, Arendash GW, Dickson A, Mamcarz MB, Lin X, Ethell DW. Abeta-specific Th2 cells provide cognitive and pathological benefits to Alzheimer's mice without infiltrating the CNS. *Neurobiol Dis* 2009; 34: 63–70.
- Dansokho C, Ait Ahmed D, Aid S, Toly-Ndour C, Chaigneau T, Calle V, et al. Regulatory T cells delay disease progression in Alzheimer-like pathology. *Brain* 2016; 139 (Pt 4): 1237–51.
- Delacourte A, David JP, Sergeant N, Buee L, Wattez A, Vermersch P, et al. The biochemical pathway of neurofibrillary degeneration in aging and Alzheimer's disease. *Neurology* 1999; 52: 1158–65.
- Duyckaerts C, Bennebic M, Grignon Y, Uchiyama T, He Y, Piette F, et al. Modeling the relation between neurofibrillary tangles and intellectual status. *Neurobiol Aging* 1997; 18: 267–73.
- Ethell DW, Shippy D, Cao C, Cracchiolo JR, Runfeldt M, Blake B, et al. Abeta-specific T-cells reverse cognitive decline and synaptic loss in Alzheimer's mice. *Neurobiol Dis* 2006; 23: 351–61.
- Fazilleau N, Delarasse C, Motta I, Fillatreau S, Gougeon ML, Kourilsky P, et al. T cell repertoire diversity is required for relapses in myelin oligodendrocyte glycoprotein-induced experimental autoimmune encephalomyelitis. *J Immunol* 2007; 178: 4865–75.
- Galea I, Bernardes-Silva M, Forse PA, van Rooijen N, Liblau RS, Perry VH. An antigen-specific pathway for CD8 T cells across the blood-brain barrier. *J Exp Med* 2007; 204: 2023–30.

- Garwood CJ, Cooper JD, Hanger DP, Noble W. Anti-inflammatory impact of minocycline in a mouse model of tauopathy. *Front Psychiatry* 2010; 1: 136.
- Gorlovoy P, Larionov S, Pham TT, Neumann H. Accumulation of tau induced in neurites by microglial proinflammatory mediators. *FASEB J* 2009; 23: 2502–13.
- Grober E, Dickson D, Sliwinski MJ, Buschke H, Katz M, Crystal H, et al. Memory and mental status correlates of modified Braak staging. *Neurobiol Aging* 1999; 20: 573–9.
- Guerreiro R, Wojtas A, Bras J, Carrasquillo M, Rogava E, Majounie E, et al. TREM2 variants in Alzheimer's disease. *N Engl J Med* 2013; 368: 117–27.
- Heneka MT, Carson MJ, El Khoury J, Landreth GE, Brosseron F, Feinstein DL, et al. Neuroinflammation in Alzheimer's disease. *Lancet Neurol* 2015; 14: 388–405.
- Hong S, Beja-Glasser VF, Nfonoyim BM, Frouin A, Li S, Ramakrishnan S, et al. Complement and microglia mediate early synapse loss in Alzheimer mouse models. *Science* 2016; 352: 712–16.
- Jaerve A, Müller HW. Chemokines in CNS injury and repair. *Cell Tissue Res* 2012; 349: 229–48.
- Jones L, Holmans PA, Hamshere ML, Harold D, Moskvina V, Ivanov D, et al. Genetic evidence implicates the immune system and cholesterol metabolism in the aetiology of Alzheimer's disease. *PLoS One* 2010; 5: e13950.
- Jones RS, Lynch MA. How dependent is synaptic plasticity on microglial phenotype? *Neuropharmacology* 2015; 96 (Pt A): 3–10.
- Kwan WH, van der Touw W, Heeger PS. Complement regulation of T cell immunity. *Immunol Res* 2012; 54: 247–53.
- Lambert JC, Grenier-Boley B, Chouraki V, Heath S, Zelenika D, Fievet N, et al. Implication of the immune system in Alzheimer's disease: evidence from genome-wide pathway analysis. *J Alzheimers Dis* 2010; 20: 1107–18.
- Lambert JC, Ibrahim-Verbaas CA, Harold D, Naj AC, Sims R, Bellenguez C, et al. Meta-analysis of 74,046 individuals identifies 11 new susceptibility loci for Alzheimer's disease. *Nat Genet* 2013; 45: 1452–8.
- Laurent C, Eddarkaoui S, Derisbourg M, Leboucher A, Demeyer D, Carrier S, et al. Beneficial effects of caffeine in a transgenic model of Alzheimer's disease-like tau pathology. *Neurobiol Aging* 2014; 35: 2079–90.
- Laurent C, Burnouf S, Ferry B, Batalha VL, Coelho JE, Baqi Y, et al. A2A adenosine receptor deletion is protective in a mouse model of Tauopathy. *Mol Psychiatry* 2016; 21: 97–107.
- Leboucher A, Laurent C, Fernandez-Gomez FJ, Burnouf S, Troquier L, Eddarkaoui S, et al. Detrimental effects of diet-induced obesity on  $\tau$  pathology are independent of insulin resistance in  $\tau$  transgenic mice. *Diabetes* 2013; 62: 1681–8.
- Liblau RS, Gonzalez-Dunia D, Wiendl H, Zipp F. Neurons as targets for T cells in the nervous system. *Trends Neurosci* 2013; 36: 315–24.
- Liu S, Liu Y, Hao W, Wolf L, Kiliaan AJ, Penke B, et al. TLR2 is a primary receptor for Alzheimer's amyloid  $\beta$  peptide to trigger neuroinflammatory activation. *J Immunol* 2012; 188: 1098–107.
- Lueg G, Gross CC, Lohmann H, Johnen A, Kemmling A, Deppe M, et al. Clinical relevance of specific T-cell activation in the blood and cerebrospinal fluid of patients with mild Alzheimer's disease. *Neurobiol Aging* 2015; 36: 81–9.
- Man SM, Ma YR, Shang DS, Zhao WD, Li B, Guo DW, et al. Peripheral T cells overexpress MIP-1 $\alpha$  to enhance its transendothelial migration in Alzheimer's disease. *Neurobiol Aging* 2007; 28: 485–96.
- Mantovani A, Sica A, Sozzani S, Allavena P, Vecchi A, Locati M. The chemokine system in diverse forms of macrophage activation and polarization. *Trends Immunol* 2004; 25: 677–86.
- Marciniak E, Faivre E, Dutar P, Alves Pires C, Demeyer D, Caillierez R, et al. The Chemokine MIP-1 $\alpha$ /CCL3 impairs mouse hippocampal synaptic transmission, plasticity and memory. *Sci Rep* 2015; 5: 15862.
- Masters CL, Simms G, Weinman NA, Multhaup G, McDonald BL, Beyreuther K. Amyloid plaque core protein in Alzheimer disease and down syndrome. *Proc Natl Acad Sci USA* 1985; 82: 4245–9.
- Minatohara K, Akiyoshi M, Okuno H. Role of immediate-early genes in synaptic plasticity and neuronal ensembles underlying the memory trace. *Front Mol Neurosci* 2016; 8: 78.
- Monsonogo A, Zota V, Karni A, Krieger JI, Bar-Or A, Bitan G, et al. Increased T cell reactivity to amyloid beta protein in older humans and patients with Alzheimer disease. *J Clin Invest* 2003; 112: 415–22.
- Monsonogo A, Imitola J, Petrovic S, Zota V, Nemirovsky A, Baron R, Fisher Y, et al. Abeta-induced meningoencephalitis is IFN-gamma-dependent and is associated with T cell-dependent clearance of Abeta in a mouse model of Alzheimer's disease. *Proc Natl Acad Sci USA* 2006; 103: 5048–53.
- Nash KR, Lee DC, Hunt JB Jr, Morganti JM, Selenica ML, Moran P, et al. Fractalkine overexpression suppresses tau pathology in a mouse model of tauopathy. *Neurobiol Aging* 2013; 34: 1540–8.
- Papegaye A, Eddarkaoui S, Deramecourt V, Fernandez-Gomez FJ, Pantano P, Obriot H, et al. Reduced Tau protein expression is associated with frontotemporal degeneration with progranulin mutation. *Acta Neuropathol Comm* 2016; 4: 74.
- Patterson SL. Immune dysregulation and cognitive vulnerability in the aging brain: interactions of microglia, IL-1 $\beta$ , BDNF and synaptic plasticity. *Neuropharmacology* 2015; 96 (Pt A): 11–18.
- Pool M, Rambaldi I, Darlington PJ, Wright MC, Fournier AE, Bar-Or A. Neurite outgrowth is differentially impacted by distinct immune cell subsets. *Mol Cell Neurosci* 2012; 49: 68–76.
- Qiao H, Foote M, Graham K, Wu Y, Zhou Y. 14-3-3 proteins are required for hippocampal long-term potentiation and associative learning and memory. *J Neurosci* 2014; 34: 4801–8.
- Rogers J, Lubner-Narod J, Styren SD, Civin WH. Expression of immune system-associated antigens by cells of the human central nervous system: relationship to the pathology of Alzheimer's disease. *Neurobiol Aging* 1988; 9: 339–49.
- Rosset MB, Lui G, Dansokho C, Chaigneau T, Dorothée G. Vaccine-induced A $\beta$ -specific CD8 $^{+}$  T cells do not trigger autoimmune neuroinflammation in a murine model of Alzheimer's disease. *J Neuroinflamm* 2015; 12: 95.
- Sasaki A, Kawarabayashi T, Murakami T, Matsubara E, Ikeda M, Hagiwara H, et al. Microglial activation in brain lesions with tau deposits: comparison of human tauopathies and tau transgenic mice TgTauP301L. *Brain Res* 2008; 1214: 159–68.
- Sauer BM, Schmalstieg WF, Howe CL. Axons are injured by antigen-specific CD8 $^{+}$  T cells through a MHC class I- and granzyme B-dependent mechanism. *Neurobiol Dis* 2013; 59: 194–205.
- Schindowski K, Bretteville A, Leroy K, Bégard S, Brion JP, Hamdane M, et al. Alzheimer's disease-like tau neuropathology leads to memory deficits and loss of functional synapses in a novel mutated tau transgenic mouse without any motor deficits. *Am J Pathol* 2006; 169: 599–616.
- Sergeant N, Bretteville A, Hamdane M, Caillet-Boudin ML, Grognet P, Bombois S, et al. Biochemistry of tau in Alzheimer's disease and related neurological disorders. *Expert Rev Proteomics* 2008; 5: 207–224.
- Shechter R, Miller O, Yovel G, Rosenzweig N, London A, Ruckh J, et al. Recruitment of beneficial M2 macrophages to injured spinal cord is orchestrated by remote brain choroid plexus. *Immunity* 2013; 38: 555–69.
- Stalder AK, Ermini F, Bondolfi L, Krenger W, Burbach GJ, Deller T, et al. Invasion of hematopoietic cells into the brain of amyloid precursor protein transgenic mice. *J Neurosci* 2005; 25: 11125–32.
- Togo T, Akiyama H, Iseki E, Kondo H, Ikeda K, Kato M, et al. Occurrence of T cells in the brain of Alzheimer's disease and other neurological diseases. *J Neuroimmunol* 2002; 124: 83–92.

- Trifilo MJ, Bergmann CC, Kuziel WA, Lane TE. CC chemokine ligand 3 (CCL3) regulates CD8(+)-T-cell effector function and migration following viral infection. *J Virol* 2003; 77: 4004–14.
- Troquier L, Caillierez R, Burnouf S, Fernandez-Gomez FJ, Grosjean ME, Zommer N, et al. Targeting phospho-Ser422 by active Tau immunotherapy in the THYTau22 mouse model: a suitable therapeutic approach. *Curr Alzheimer Res* 2012; 9: 397–405.
- Van der Jeugd A, Ahmed T, Burnouf S, Belarbi K, Hamdane M, Grosjean ME, et al. Hippocampal tauopathy in tau transgenic mice coincides with impaired hippocampus-dependent learning and memory, and attenuated late-phase long-term depression of synaptic transmission. *Neurobiol Learn Mem* 2011; 95: 296–304.
- Van der Jeugd A, Vermaercke B, Derisbourg M, Lo AC, Hamdane M, Blum D, et al. Progressive age-related cognitive decline in tau mice. *J Alzheimers Dis* 2013; 37: 777–88.
- Vidal M, Morris R, Grosveld F, Spanopoulou E. Tissue-specific control elements of the Thy-1 gene. *EMBO J* 1990; 9: 833–40.
- Wilson EH, Weninger W, Hunter CA. Trafficking of immune cells in the central nervous system. *J Clin Invest* 2010; 120: 1368–79.
- Yoshiyama Y, Higuchi M, Zhang B, Huang SM, Iwata N, Saido TC, et al. Synapse loss and microglial activation precede tangles in a P301S tauopathy mouse model. *Neuron* 2007; 53: 337–51.
- Zotova E, Bharambe V, Cheaveau M, Morgan W, Holmes C, Harris S, et al. Inflammatory components in human Alzheimer's disease and after active amyloid- $\beta$ 42 immunization. *Brain* 2013; 136: 2677–96.